Respiratory Research

RESEARCH

Open Access

Integrin α8 is a useful cell surface marker of alveolar lipofibroblasts

Atsuki Fukada[1,2], Yasunori Enomoto[1*], Ryo Horiguchi[3], Yoichiro Aoshima[1,4], Shiori Meguro[1], Hideya Kawasaki[5], Isao Kosugi[1], Tomoyuki Fujisawa[2], Noriyuki Enomoto[2], Naoki Inui[2], Takafumi Suda[2] and Toshihide Iwashita[1]

Abstract

Background Recent advances in comprehensive gene analysis revealed the heterogeneity of mouse lung fibroblasts. However, direct comparisons between these subpopulations are limited due to challenges in isolating target subpopulations without gene-specific reporter mouse lines. In addition, the properties of lung lipofibroblasts remain unclear, particularly regarding the appropriate cell surface marker and the niche capacity for alveolar epithelial cell type 2 (AT2), an alveolar tissue stem cell.

Methods and results Using cell surface markers applicable even into wild-type mouse lungs, we could classify PDGFRα$^+$ total lung resident fibroblasts into at least two major distinct subpopulations: integrin α8 (ITGA8)$^+$ and SCA-1$^+$ fibroblasts. We analyzed their characteristics, including lipid content, transcriptome profiles, and alveolar stem cell niche capacity. ITGA8$^+$ fibroblasts showed higher positivity of intracellular lipid droplets compared to SCA-1$^+$ fibroblasts (91.0 ± 1.5% vs. 5.0 ± 0.5% in LipidTOX staining; 91.3 ± 1.4% vs. 7.1 ± 1.7% in Oil Red O staining). The fluorescence intensity of LipidTOX in the ITGA8$^+$ fibroblasts was highest in newborn compared to adult or aged lungs. The transcriptome profile of ITGA8$^+$ fibroblasts in adult mouse lungs, evaluated through two independent single-cell RNA-seq datasets, consistently showed higher expression of *Tcf21* and *Plin2*, which are canonical markers of lipofibroblasts. ITGA8$^+$ fibroblasts were primarily located in the alveolar area, particularly in the neighborhood of AT2. Compared to SCA-1$^+$ fibroblasts, ITGA8$^+$ fibroblasts showed higher mRNA expression of potential AT2-supportive factors, *Fgf10*, *Fgf7*, and *Wnt2*, but unexpectedly, exhibited lower efficiency in alveolar organoid formation.

Conclusions ITGA8$^+$ lung fibroblasts correspond to alveolar lipofibroblasts, but the alveolar niche capacity may be lower than SCA-1$^+$ lung fibroblasts. Further studies are necessary for the functional distinction between lung fibroblast subpopulations.

Keywords Lung fibroblast, Lipofibroblast, Single cell RNA-seq, ITGA8, SCA-1

*Correspondence:
Yasunori Enomoto
enomotoy@hama-med.ac.jp
[1]Department of Regenerative and Infectious Pathology, Hamamatsu University School of Medicine, 1-20-1 Handayama Chuo-ku, Hamamatsu, Shizuoka 431-3192, Japan
[2]Second Division, Department of Internal Medicine, Hamamatsu University School of Medicine, Hamamatsu, Japan
[3]Advanced Research Facilities and Services, Hamamatsu University School of Medicine, Hamamatsu, Japan
[4]Department of Respiratory Medicine, Iwata City Hospital, Iwata, Japan
[5]Preeminent Medical Photonics Education and Research Center Institute for NanoSuit Research, Hamamatsu University School of Medicine, Hamamatsu, Japan

Introduction

The lung consists of a conducting airway and a respiratory portion, both surrounded by interstitium or interstitial connective tissue. Fibroblasts are the most common cells in the lung interstitium and are responsible for the formation and maintenance of interstitial fibers (collagen and elastic fibers) and matrix, as well as the signaling niches to the surrounding cells [1–3]. Alveoli, which is a minimum unit of respiratory portion, is covered by two types of alveolar epithelial cells, known as type 1 (AT1) and type 2 (AT2), and AT2 is a tissue stem cell in alveoli and can self-renew and differentiate into AT1. Alveolar fibroblasts, mainly *Pdgfra*$^{+}$ lung fibroblasts, mechanically and functionally supports AT2 as a stem cell niche [4]. Therefore, any fibroblast abnormality can lead to lung diseases with AT2 disorders, including pulmonary fibrosis [5, 6]. This underscores the importance of studying this cell type.

Recent technological advances, particularly due to single-cell RNA sequencing (scRNA-seq), have broaden our scientific knowledge regarding the heterogeneity of lung resident fibroblasts and identified several subpopulations based on the transcriptome profiles. Lee et al. analyzed lung mesenchymal cells in the view of *Lgr5* or *Lgr6* lineage and reported the AT2-supportive capacity of *Lgr5*$^{+}$ mesenchymal cells [7]. Zepp et al. proposed a novel lung mesenchymal subpopulation, termed as mesenchymal alveolar niche cell (MANC), which also successfully supported AT2 [8]. Taghizadeh et al. also proposed another AT2-supportive subpopulation, SCA-1^{+}*Fgf10*$^{+}$ mesenchymal cell [9]. Xie et al. categorized resident fibroblasts in untreated lungs into lipofibroblast, *Col13a1*$^{+}$ fibroblast, and *Col14a1*$^{+}$ fibroblast [10]. Although in the same group, Liu et al. newly determined fibroblast subpopulations, lipofibroblast, *Ebf1*$^{+}$ fibroblast, proliferating fibroblasts, myofibroblast (in developing lungs), and intermediate subtype [11]. Tsukui et al. analyzed the *Col1a1-GFP* mouse lungs and found at least three fibroblast subpopulations in their untreated lungs: alveolar lipofibroblast, adventitial fibroblast, and peribronchial fibroblast [12]. However, the overlap and distinction between these many proposed subpopulations are unclear due to differences in mouse lines used. Additionally, most subpopulations were determined only based on the transcriptome profiles with or without localization data, often lacking functional analysis. The live cell isolation of target subpopulations, particularly applicable even in wild-type mice, would be helpful to resolve such problems due to its ease of application and validation.

Lipofibroblasts are a fibroblast subpopulation with many lipid droplets in the cytoplasm, which is believed to transfer lipids to AT2 for surfactant synthesis [13]. Although several gene markers for lipofibroblasts have been suggested, such as *Plin2*, *Lpl*, *Tcf21*, and *Apoe* [10–12, 14–16], their coding proteins and antibodies are not generally used for live cell isolation on fluorescence-activated cell sorting (FACS). To our knowledge in the literature, potential cell surface markers for lipofibroblasts include PDGFRα, THY-1, and SCA-1 [4, 9, 17].

Previously, using wild-type mice, we demonstrated that lung resident fibroblasts could be divided into at least two subpopulations using cell surface markers, integrin α8 (ITGA8) and SCA-1 [18]. In this current study, we analyzed lung fibroblast subpopulations based on the expressions of the two markers in terms of (1) compatibility as lipofibroblasts by directly evaluating their intracellular lipid content; (2) comparison with several subpopulations proposed in previous studies using two independent scRNA-seq datasets; (3) alveolar stem cell niche capacity using an alveolar organoid assay.

Methods

All the experiments have been newly performed and the data in the present study is independent from that of our previous study [18].

Mouse lines

We obtained wild-type C57BL/6 mice from Japan SLC. We also purchased *Pdgfra-GFP* mice (B6.129S4-Pdgfra$^{tm11(EGFP)Sor}$/J; Strain #007669) [19], *Sftpc-creERT2* mice (B6.129 S-*Sftpc*$^{tm1(cre/ERT2)Blh}$/J; Strain #028054) [20], and*tdTomato*mice(B6.Cg-*Gt(ROSA)26Sor*$^{tm14(CAG-tdTomato)Hze}$/J; Strain #007914) [21] from The Jackson Laboratory. All mice were bred and kept in a specific pathogen-free mouse facility under constant temperature (18°–23 °C) and humidity (40–60%) in sterilized plastic cages. A 12 h-light/12 h-dark cycle was maintained. Typically, we utilized adult male mice aged 8–14 weeks, unless otherwise specified. To label AT2 cells, *Sftpc-creERT2; tdTomato* mice were intraperitoneally injected with tamoxifen (0.25 mg per g body weight in peanuts oil) two times on alternative days and these mice were used for organoid experiments two weeks after the last injection.

Preparation of mouse primary cells and FACS sorting

The procedure was based on that in previous studies [6, 22]. In brief, mice were euthanized, and then a perfusion of 5 mL of Dulbecco's phosphate-buffered saline (DPBS) was conducted through the right ventricle. Subsequently, 1 mL of protease solution containing Collagenase type I (900 U/mL, Worthington), Elastase (1 U/mL, Worthington), and DNaseI (0.1 mg/mL, SIGMA) in advanced DMEM was intratracheally injected, and the trachea was tied off. After a 3-min incubation on a dish, only lung lobes were extracted. These lobes were finely chopped with a small blade and incubated in 3 mL of protease solution for 45 min at 37 °C. The tissues were

then dissociated by repetitive pipetting, and 10 mL of our FACS buffer (consisting of 3% heat-inactivated FBS in DPBS) was added. The resulting cell suspension was filtered through 70 μm and 40 μm strainers. After a centrifugation step (400 g, 3 min), the cells were incubated with RBC lysis buffer (BioLegend #420301) at room temperature for 3 min. Next, the cells were resuspended in FACS buffer and centrifuged (400 g, 5 min). Following this, the cells were stained with the specified antibodies (*see* Table 1) and sorted using Moflo Astrios EQ (Beckman Coulter). The digestion procedure was common regardless of the target cells except for the combination of antibodies applied. For the organoid experiments, lung fibroblasts were isolated from *Pdgfra-GFP* mice [DAPI-negative (alive) & $GFP^+EpCAM^-CD31^-CD45^-CD146^-LYVE\text{-}1^-$] or from wild-type mice [SYTOX Red-negative (alive) & $PDGFR\alpha^+EpCAM^-CD31^-CD45^-CD146^-LYVE\text{-}1^-$] with/without selected markers (ITGA8 and SCA-1)]. AT2 cells were isolated from tamoxifen-treated *Sftpc-creERT2; tdTomato* mice [DAPI-negative (alive) & $Tomato^+EpCAM^+CD31^-CD45^-$]. For the evaluation of lipid content in each subpopulation of lung fibroblasts, wild-type C57BL/6 mice, not *Pdgfra-GFP* mice, were used due to the limitation of the fluorescence colors available, and the lung fibroblasts were determined by a panel of $PDGFR\alpha^+EpCAM^-CD31^-CD45^-CD146^-LYVE\text{-}1^-$ with/without selected markers (ITGA8, SCA-1, and THY-1). Data collection was performed using Summit Software v6.3.1 (Beckman Coulter) and FlowJo v10.7.2 was employed for the analysis of all FACS data.

Note: in evaluating or sorting fibroblasts, the lineage marker set for negative selection included CD146 (a marker of pericytes and smooth muscle cells) and LYVE-1 (lymphatic endothelial cells) in addition to CD31 (endothelial cells), CD45 (blood cells), and EpCAM (epithelial cells), which enabled to increase the purity of fibroblasts (Supplementary Fig. 1A).

Table 1 Antibodies and staining materials used in the present study

Target protein	Supplier	Code	Application	Dilution
ITGA 8 (biotin-conjugated)	R&D	BAF4076	FACS/IHC	1:100
Ly6a (SCA-1) (PE/Cy7)	eBioscience	25-5981-82	FACS	1:100
CD140a (PDGFRA) (BV421)	BioLegend	135923	FACS	1:50
CD326 (EpCAM) (APC or PE/Cy7)	eBioscience	17-5791-82	FACS	1:100
CD31 (APC or PE/Cy7)	BioLegend	102410	FACS	1:100
CD45 (APC or PE/Cy7)	BioLegend	103112	FACS	1:100
CD146 (APC)	BioLegend	134712	FACS	1:100
LYVE-1 (APC)	R&D	FAB2125A	FACS	1:100
CD90.2 (THY-1.2) (biotin-conjugated)	BioLegend	140314	FACS	1:100
PE Streptavidin	BioLegend	405203	FACS	1:100
Ly6a (Sca-1)	Miltenyi Biotec	130-123-848	IHC	1:100
Prosurfactant prontein C	Merck	AB3786	IHC	1:500
DAPI	Nakalai	19178-91	FACS/IHC	1:500
SYTOX Red	Thermo Fisher	S34859	FACS	1:1000

Culture of alveolar organoids

Sorted AT2 cells from tamoxifen-treated *Sftpc-creERT2; tdTomato* mouse lungs and lung fibroblasts from *Pdgfra-GFP* or wild-type mouse lungs were mixed in culture medium, along with an equal volume of growth factor-reduced Matrigel™ (Corning #354230). We placed 800 AT2 cells and 4000 fibroblasts per 20 μL gel-containing drop at the bottom of 24-well plates. These drops were allowed to solidify by incubating for 20 min at 37 °C, after which 500 μL of medium was added to each well. The culture medium composition was as follows: 50 ng/mL human EGF (ThermoFisher #PHG0311), 30 μg/mL Bovine Pituitary Extract (ThermoFisher #13028014), 5 μg/mL heparin (Merck #H3149-100KU), 10 μM Y-27632 (FUJIFILM #030-24021), GlutaMAX Supplement (Gibco #35050-061), Insulin-Transferrin-Selenium (Gibco #41400045) in Advanced DMEM (Thermo Fisher #12491015) containing 5% FBS. The medium remained unchanged until day 11. Organoids were imaged using CellDiscoverer 7 (Carl Zeiss). The number and size were evaluated only for $Tomato^+$ organoids with a diameter more than 50 μm. For the isolation of AT2-derived cells from Matrigel™, only live $Tomato^+$ cells (without DAPI positivity) were sorted after dissolving the gel using TrypLE™ Express Enzyme (Gibco #12605010) for 30 min.

Immunohistochemistry

Sections were stained with primary antibodies listed in Table 1. Secondary antibodies directly conjugated with Alexa Fluor 488/555/647 were used for multi-color imaging. DAPI was used for nuclear counter staining. Images were obtained using a TCS SP8 confocal microscope (Leica). The distance between cells was defined as the distance between the center of DAPI-positive nuclei in each cell. For the measurement, z-stacks and the projection images were acquired from at least three different sections from three individual mice.

Evaluation of lipid content

Lipid content was evaluated using LipidTOX (HCS LipidTox™ Green Neutral Lipid Stain: Invitrogen #H34475; dilution 1:200) and Oil Red O (MutoPureChemicals #40492) after FACS with Cytospin preparation. For LipidTOX staining, fixation with 4% paraformaldehyde and

permeabilization with 4% saponin were performed, and fluorescence was evaluated by TCS SP8 confocal microscope (Leica). For Oil Red O staining, fixation with 4% paraformaldehyde and incubation with 60% isopropanol were done, followed by staining with 60% Oil red O working solution with/without Hematoxylin counterstain. The images of Oil Red O were obtained using IX83 inverted microscope (Olympus). The visualized lipid droplets (stained by LipidTOX or Oil Red O) in each cell were semi-quantitatively scored: absent (LipidTOX) or scarce (Oil Red O) = score 0; a few = score 1; many = score 2. The representative images are shown in Fig. 1B and C. The scoring was performed to 300 cells in each fibroblast subpopulation in a mouse lung and the sum of the semi-quantitative scores was also calculated. The binary cutoff of "presence of intracellular lipid" was defined as the score with 1 or 2. The quantification of mean fluorescence intensity of LipidTOX in each target subpopulation was evaluated using flow cytometry.

scRNA-seq library preparation, sequencing, and data processing

Lung cells were obtained from three 12-week-old male wild-type mice, and these cells constituted one sample. Using FACS, we sorted live (SYTOX Red-negative) lineage-negative cells (negative for E-cadherin, CD45, CD31, CD146, LYVE-1, and TER119) and loaded them onto the Chromium controller (10x Genomics). For library preparation, we utilized the Chromium Next GEM Single Cell 3′ Kit v3.1 according to the

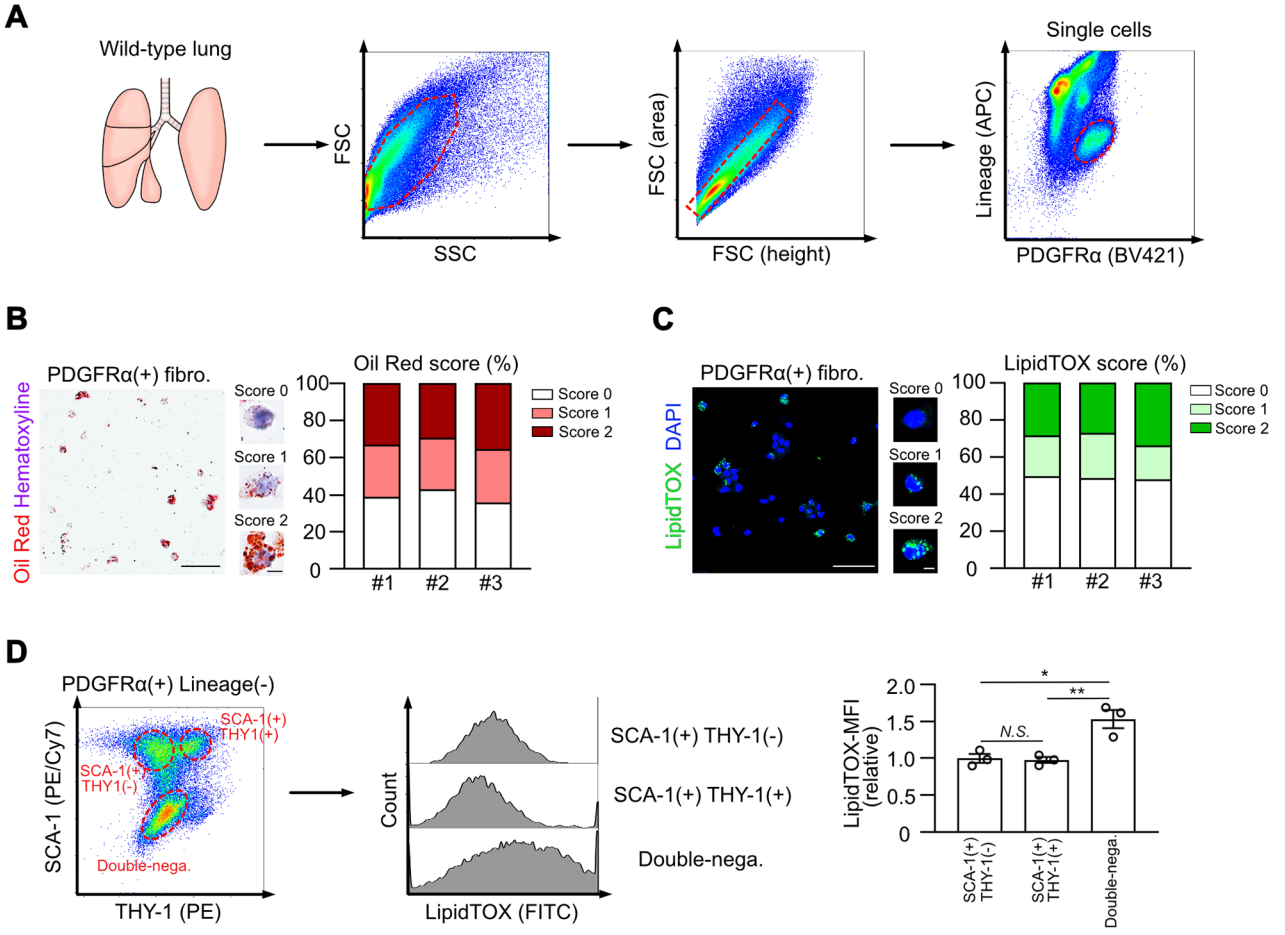

Fig. 1 Evaluation of previously-reported cell surface markers for lung lipofibroblasts. (**A**) Representative FACS gating panels for sorting PDGFRα$^+$ lung fibroblasts. Lineage = a mixture of EpCAM (for epithelial cells), CD31 (endothelial cells), CD45 (blood cells), CD146 (smooth muscle cells and pericytes), and LYVE-1 (lymphatic endothelial cells). (**B**) Representative images of PDGFRα$^+$ lung fibroblasts on Oil Red O staining and the scoring result (*scale bar: left = 50 μm; right = 5 μm*). The results are obtained from three independent adult male mice (wild-type: #1, #2, and #3). (**C**) Representative images of PDGFRα$^+$ lung fibroblasts on LipidTOX staining and the scoring result (*scale bar: left = 50 μm; right = 5 μm*). The results are obtained from three independent adult male mice (wild-type: #1, #2, and #3). (**D**) FACS panels of PDGFRα$^+$ lung fibroblasts and LipidTOX-fluorescence intensities between SCA-1$^+$THY-1$^-$, SCA-1$^+$THY-1$^+$, and double-negative cells. The right graph is the quantification. Data represent the mean ± SEM of results obtained from three independent adult male mice (wild-type). *$P < 0.05$, **$P < 0.01$ (one-way analysis of variance with Bonferroni correction). Lineage = a mixture of EpCAM, CD31, CD45, CD146, and LYVE-1

manufacturer's protocol. The libraries were sequenced on DNBSEQ-G400 (MGI). Sequencing data were aligned to the mouse genome mm10 using CellRanger version 6.1.1 (10x Genomics). Data processing was performed using the Seurat R package version 4.0.5. Cells with fewer than 200 genes detected or greater than 10% mitochondria genes were excluded. Clustering was done using the FindClusters function of Seurat (dims.use = 1:20). Cluster visualization on a 2D map was achieved through uniform manifold approximation and projection (UMAP) (using the RunUMAP function of Seurat, dims.use = 1:20). UMAP plots and dot plots were generated using Seurat.

RNA velocity estimation

The spliced (exonic) and unspliced (intronic) transcript levels were determined from the CellRanger version 6.1.1 (10x Genomics) output using Velocyto version 0.17.17 (run10x function) [23]. RNA velocity was estimated in stochastic mode from the resulting unspliced/spliced count loom file and visualized with scVelo version 0.2.4 [24].

Total RNA isolation, cDNA preparation, and quantitative RT-PCR

Total RNA was purified with ISOGEN (NIPPON GENE) as per the manufacturer's instructions. Then, it was reverse transcribed to cDNA by SuperScript III First-strand synthesis system (INVITROGEN) according to manufacturer's instructions. Quantitative RT-PCR was performed using primer sets shown in Table 2, utilizing Thunderbird SYBR qPCR mix (TOYOBO) on QuantStudio5 Real-time PCR machine (Thermo Fisher Scientific). PCR cycling parameters were 95 °C for 10 min (one cycle); 95 °C for 15 s and 60 °C for 60 s (40 cycles). *Gapdh* (glyceraldehyde 3-phosphate dehydrogenase) was used for the normalization of gene expression as a house-keeping gene. Fold-changes in expression of targeted genes were calculated using $2^{-\Delta\Delta Ct}$ method.

Table 2 Primers used in the present study

Gene	Forward	Reverse
Gapdh	AACTTTGGCATTGTGGAAGG	GGATGCAGGGATGATGTTCT
Fgf7	TTTGGAAAGAGCGACGACTT	GGCAGGATCCGTGTCAGTAT
Fgf10	GCCACCAACTGCTCTTCTTC	CTGACCTTGCCGTTCTTCTC
Wnt2	ATCTCTTCAGCTGGCGTTGT	CCTTCCTTCCAGCTCTGTTG
Tcf21	CAAACCCAACACACGAAGTG	GTCACAGTCCAGCATCTCCA
Plin2	CCCTGTCTACCAAGCTCTGC	CGATGCTTCTCTTCCACTCC
Npnt	GACGTGGTCAAAGGACAGGT	CTCTTCCAGTCGCACATTCA
Epcam	GAGTCCGAAGAACCGACAA GGA	GATGTGAACGCCTCTTGA AGCG
Sftpc	GTCCTCGTTGTCGTGGTGATTG	AAGGTAGCGATGGTGTCT GCTC
Pdpn	ACAACCACAGGTGCTACTGGAG	GTTGCTGAGGTGGACAG TTCCT
Krt8	AGATCACCACCTACCGCAAG	TGAAGCCAGGGCTAGTG AGT
Mki67	GACAGCTTCCAAAGCTCACC	TGTGTCCTTAGCTGCCTCCT

Reanalysis of datasets of single-cell RNA-seq

Re-analysis for single-cell RNA-seq datasets was performed using R studio software using the Seurat package (https://satijalab.org/seurat/index.html).

Human lung samples

Formalin-fixed human lung samples were collected from six adult subjects, who received autopsy at Hamamatsu University Hospital and had not been diagnosed with lung diseases including emphysema, fibrosis, or cancer. Using the frozen sections, LipidTOX was stained.

Data availability

The authors declare that all data supporting the findings of this study are available within the article and its supplementary materials. Our original sequencing data in this study are available at NCBI GEO under the accession numbers GSE244237. Previously published sequencing data that were reanalyzed are available under the accession number GSE132771 (mouse: integrated data of GFP^+ and GFP^- cells; human: integrated data of "NML1_ALL", "NML2_ALL", and "NML3_ALL") [12].

Statistics

All results are presented as mean ± standard error (SEM) from a minimum of three independent mice. Statistical analyses were performed using unpaired Student's t-test (two-tailed) for comparisons between two groups or using a one-way analysis of variance with Bonferroni correction for comparisons between more than two groups. The differences with $P < 0.05$ are considered significant.

Results

ITGA8 is a useful cell surface marker for lung lipofibroblasts

PDGFRα is a pan-fibroblast marker in the lungs that can be used for cell sorting (Fig. 1A). To evaluate the actual lipid content in the $PDGFR\alpha^+$ fibroblasts, direct visualization using LipidTOX and Oil Red O staining was done and revealed that about 40% of $PDGFR\alpha^+$ fibroblasts did not have apparent lipid droplets in their cytoplasm (Fig. 1B and C), suggesting that the expression of PDGFRα is not specific for lipofibroblasts. Among $PDGFR\alpha^+$ fibroblasts, another potential lipofibroblast markers, THY-1 and SCA-1 [9, 17], were evaluated but did not guarantee high or frequent lipid content (Fig. 1D and Supplementary Fig. 1B). Even when evaluating $THY\text{-}1^+$ or $SCA1^+$ cells in all cell types, not just fibroblasts, the intracellular lipid was rarely seen (Supplementary Fig. 1C). Collectively, PDGFRα, THY-1, and SCA-1 seemed not suitable for a marker of lipofibroblasts.

PDGFRα$^+$ total lung resident fibroblasts were divided by the protein expressions of ITGA8 and SCA-1 using FACS, as we have previously reported (*Correction from our previous paper: the expression of SCA-1 in the ITGA8-single-positive fibroblasts was mainly "negative", not "low"*) [18]. More detailed evaluation by flow cytometry revealed that PDGFRα$^+$ fibroblasts were subdivided into three groups: SCA-1-single-positive, SCA-1&ITGA8-double-positive, and ITGA8-single-positive fibroblasts. Furthermore, it was found that the expression of PDGFRα protein increased in this order (Supplementary Fig. 2A). Then, it was determined whether this dividing method can be used for lipofibroblast identification. Interestingly, ITGA8-single-positive fibroblasts showed more lipid score and higher lipid droplet positivity than SCA-1-single-positive fibroblasts (91.0 ± 1.5% vs. 5.0 ± 0.5% in LipidTOX staining; 91.3 ± 1.4% vs. 7.1 ± 1.7% in Oil Red O staining). The double-positive fibroblasts (SCA-1$^+$ and ITGA8$^+$) showed the intermediate lipid score between SCA-1- and ITGA8-single-positive fibroblasts (Fig. 2A and B, and 2C). Even when comparing ITGA8-positive with -negative fibroblasts, the former showed significantly more intra-cellular lipid content (Supplementary Fig. 2B, 2 C, and 2D). The lipid droplet positivity in ITGA8-positive vs. -negative fibroblasts was 90.3 ± 1.2% vs. 1.6 ± 0.6% in LipidTOX staining or 92.9 ± 1.6% vs. 8.6 ± 0.7% in Oil Red O staining.

It was also found that the mean fluorescence intensity of LipidTOX in ITGA8$^+$ fibroblasts was the highest at newborn (postnatal day 7) compared to adult (2-month-old) or aged (2-year-old) lungs. In contrast, ITGA8$^+$ fibroblasts consistently had lipids in their cytoplasm even in the aged lungs (Fig. 2D). These results suggest that ITGA8 is a useful and consistent cell surface marker of mouse lung lipofibroblasts regardless of age.

Comparison of ITGA8$^+$ or SCA-1$^+$ fibroblasts with other lung fibroblast subpopulations proposed in previous studies

One of the most important functions of alveolar fibroblasts is supporting AT2, an alveolar epithelial tissue stem cell [4, 25]. In the lungs of *Pdgfra-GFP* mice, ITGA8$^+$GFP$^+$ fibroblasts were confirmed to be localized frequently at the alveolar area, particularly at the neighborhood of SFTPC-positive AT2 cells (Fig. 3A). In contrast, SCA-1$^+$GFP$^+$ or ITGA8$^-$GFP$^+$ fibroblasts were relatively flat-shaped and found mostly at the peribronchial and peri-vascular area (Fig. 3A). The distances from the nearest AT2 cells for the ITGA8$^+$GFP$^+$ fibroblasts were much shorter than for the SCA-1$^+$GFP$^+$ or ITGA8$^-$GFP$^+$ fibroblasts (*Note: 94.8 ± 1.2% of ITGA8-negative fibroblasts was positive for SCA-1 in flowcytometry, n = 3*). The mean distances were 10.0 μm, 58.7 μm, and 61.5 μm, respectively (Fig. 3B).

To evaluate the transcriptome profiles of ITGA8$^+$ and SCA-1$^+$ fibroblasts, we utilized a published dataset of scRNA-seq (GSE132771) by Tsukui et al., which analyzed untreated adult mouse lungs. [12] Consistent with our FACS results, *Pdgfra*$^+$ lung fibroblasts could be divided into two major subpopulations: *Itga8*$^+$ or *Ly6a*$^+$ (a SCA-1 gene) fibroblasts when the analysis resolution was set at a low level (Fig. 3C). Except for fibroblasts, the expressions of *Itga8* and *Ly6a* were mainly observed in smooth muscle cells and endothelial cells, respectively (Supplementary Fig. 3). Based on the transcriptome comparison, *Itga8*$^+$ fibroblasts showed higher mRNA expressions of AT2-supportive factors [9, 25–27], such as *Fgf10*, *Fgf7*, and *Wnt2* (Fig. 3C). They also had higher expressions of *Tcf21*, *Plin2*, *Col13a1*, and *Npnt*, which are similar to those of "lipofibroblast" determined by Liu et al. [11], "alveolar lipofibroblast" by Tsukui et al. [12], and "*Col13a1*$^+$ fibroblast" by Xie et al. [10]. Additionally, we confirmed the reproducibility even in the FACS-sorted lung fibroblasts of *Pdgfra-GFP* mice by qRT-PCR analyses of selected genes (Supplementary Fig. 4). In contrast, *Ly6a* (SCA-1)$^+$ fibroblasts showed a signature resembling a mixture of several proposed subpopulations in each study, such as, "*Col14a1*$^+$ fibroblast (the major genes: *Col14a1* and *Pi16*)" and "lipofibroblast (*Cd44* and *Cd9*)" defined by Xie et al. [10]; "*Ebf1*$^+$ fibroblast (*Ebf1* and *Pdgfrb*)" and "intermediate subtype (*Igfbp7* and *Fbln5*)" by Liu et al. [11]; "peribronchial fibroblast (*Hhip* and *Aspn*)" and "adventitial fibroblast (*Col14a1* and *Pi16*)" by Tsukui et al. [12] (Fig. 3C). To validate these findings, we originally performed scRNA-seq using wild-type mouse lung-derived, lineage marker (CD45/CD31/E-cadherin/CD146/LYVE-1/TER119)-negative, FACS-sorted mesenchymal cells (GSE244237). Similar results were reproduced even in our dataset (Fig. 3D and Supplementary Fig. 5). Interestingly, an RNA velocity analysis suggested that *Ly6a*$^+$ fibroblasts were in more progenitor status than *Itga8*$^+$ fibroblasts (Supplementary Fig. 6).

In contrast, in both the scRNA-seq datasets, we could not confidently determine which clusters correspond to some of the previously-reported AT2-supportive fibroblast subpopulations, *Lgr5*$^+$ mesenchymal cell (due to the extremely-low expression level of *Lgr5* or *Lgr6* among the *Pdgfra*$^+$ total lung fibroblasts) [7], MANC (due to the inconsistent expression pattern regarding the reported major marker genes, such as *Axin2*, *Mmp2*, and *Sfrp4*) [8], and SCA-1$^+$*Fgf10*$^+$ mesenchymal cell (due to the low expression level of *Fgf10* in *Ly6a*$^+$ fibroblasts) [9], regardless of the resolution level analyzed (Supplementary Figs. 3 and 5).

Evaluation of alveolar stem cell niche capacity

Although the localization data and transcriptome profiles suggested a higher alveolar stem cell niche capacity for

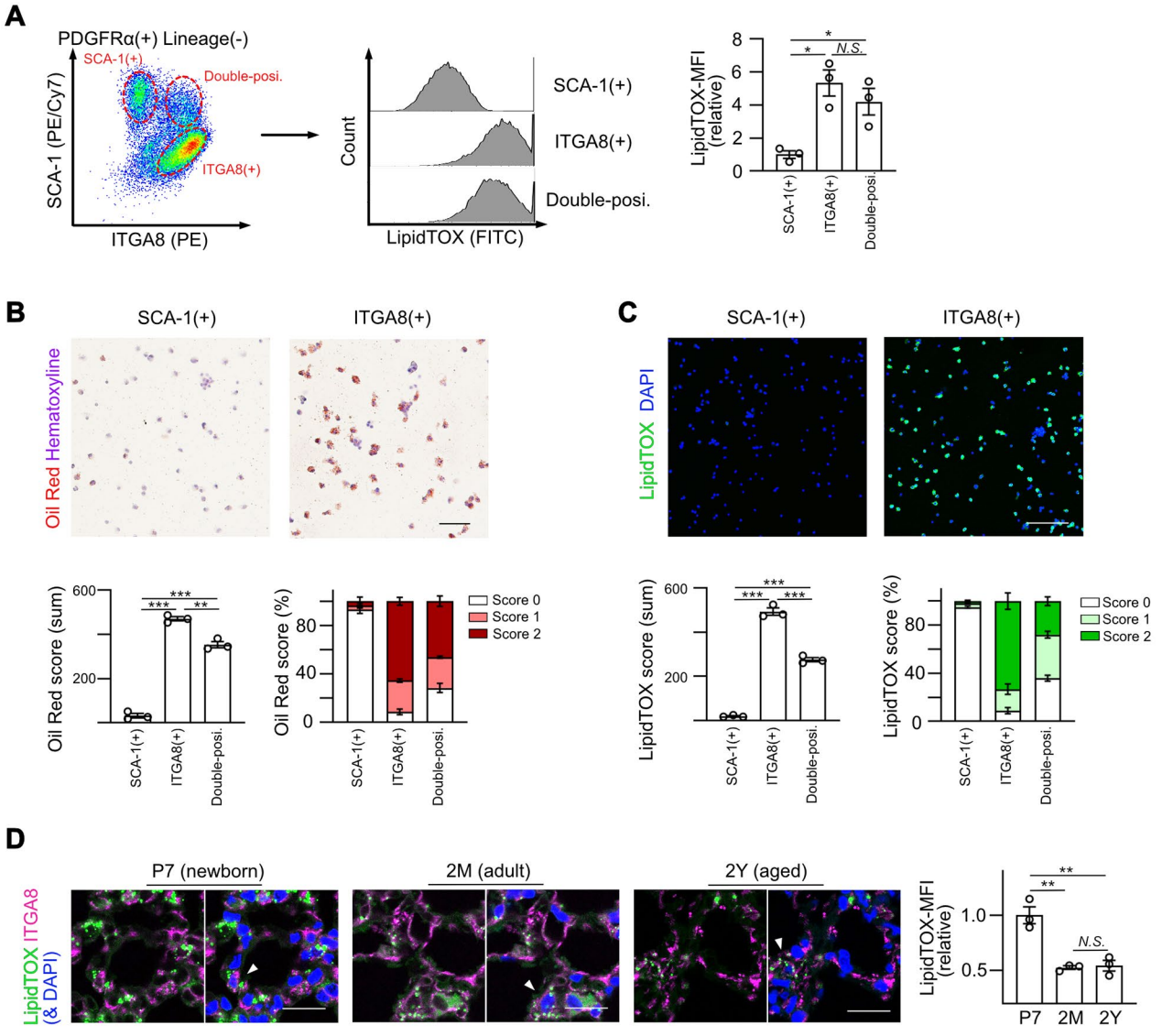

Fig. 2 Evaluation of ITGA8 as a cell surface marker for lung lipofibroblasts. (**A**) FACS panels of PDGFRα$^+$ lung fibroblasts and LipidTOX-fluorescence intensities between SCA-1-single-positive, ITGA8-single-positive, and double-positive fibroblasts. The right graph is the quantification. Data represent the mean ± SEM of results obtained from three independent adult male mice (wild-type). *$P < 0.05$ (one-way analysis of variance with Bonferroni correction). Lineage = a mixture of EpCAM, CD31, CD45, CD146, and LYVE-1. *Note: ITGA8 was also expressed in non-fibroblast cells (CD31-positive cells: 5.2% in average; CD45-positive cells: 1.9%; CD146-positive cells: 4.4%; EpCAM-positive cells: 0.7%)* ($n = 3$, *wild-type adult male mice*). (**B**) Representative images of Oil Red O staining with hematoxyline for SCA-1-single-positive and ITGA8-single-positive lung fibroblasts (*scale bar: 50 μm*) and the quantification including double-positive fibroblasts (sum and breakdown of the scores). Data represent the mean ± SEM of results obtained from three independent adult male mice (wild-type). **$P < 0.01$, ***$P < 0.001$ (one-way analysis of variance with Bonferroni correction). (**C**) Representative images of LipidTOX staining with DAPI (*scale bar: 100 μm*) for SCA-1-single-positive and ITGA8-single-positive lung fibroblasts and the quantification including double-positive fibroblasts (sum and breakdown of the scores). Data represent the mean ± SEM of results obtained from three independent adult male mice (wild-type). ***$P < 0.001$ (one-way analysis of variance with Bonferroni correction). (**D**) Representative images of newborn (P7), adult (2 months), and aged (2 years) lungs stained with LipidTOX, anti-ITGA8 antibody, and DAPI (*scale bars: 20 μm*), and the quantification of LipidTOX-fluorescence intensities of ITGA8$^+$ lung fibroblasts evaluated by flowcytometry. Triangles show ITGA8$^+$LipidTOX$^+$ fibroblasts. Data represent the mean ± SEM of results obtained from three independent mice (wild-type) in each generation. **$P < 0.01$ (one-way analysis of variance with Bonferroni correction)

ITGA8$^+$ fibroblasts, these findings were based on indirect evidence. To confirm these, an alveolar organoid assay was conducted using AT2 from tamoxifen-treated *Sftpc-creERT2; tdTomato* mice and lung fibroblasts from *Pdgfra-GFP* or wild-type mice. Here, three subpopulations of lung fibroblasts within the same lung were sorted and compared: ITGA8-single-positive fibroblasts (ITGA8$^+$SCA-1$^-$GFP$^+$), SCA-1-single-positive fibroblasts (SCA-1$^+$ITGA8$^-$GFP$^+$), and double-positive fibroblasts (ITGA8$^+$SCA-1$^+$GFP$^+$) (Fig. 4A). Results showed that

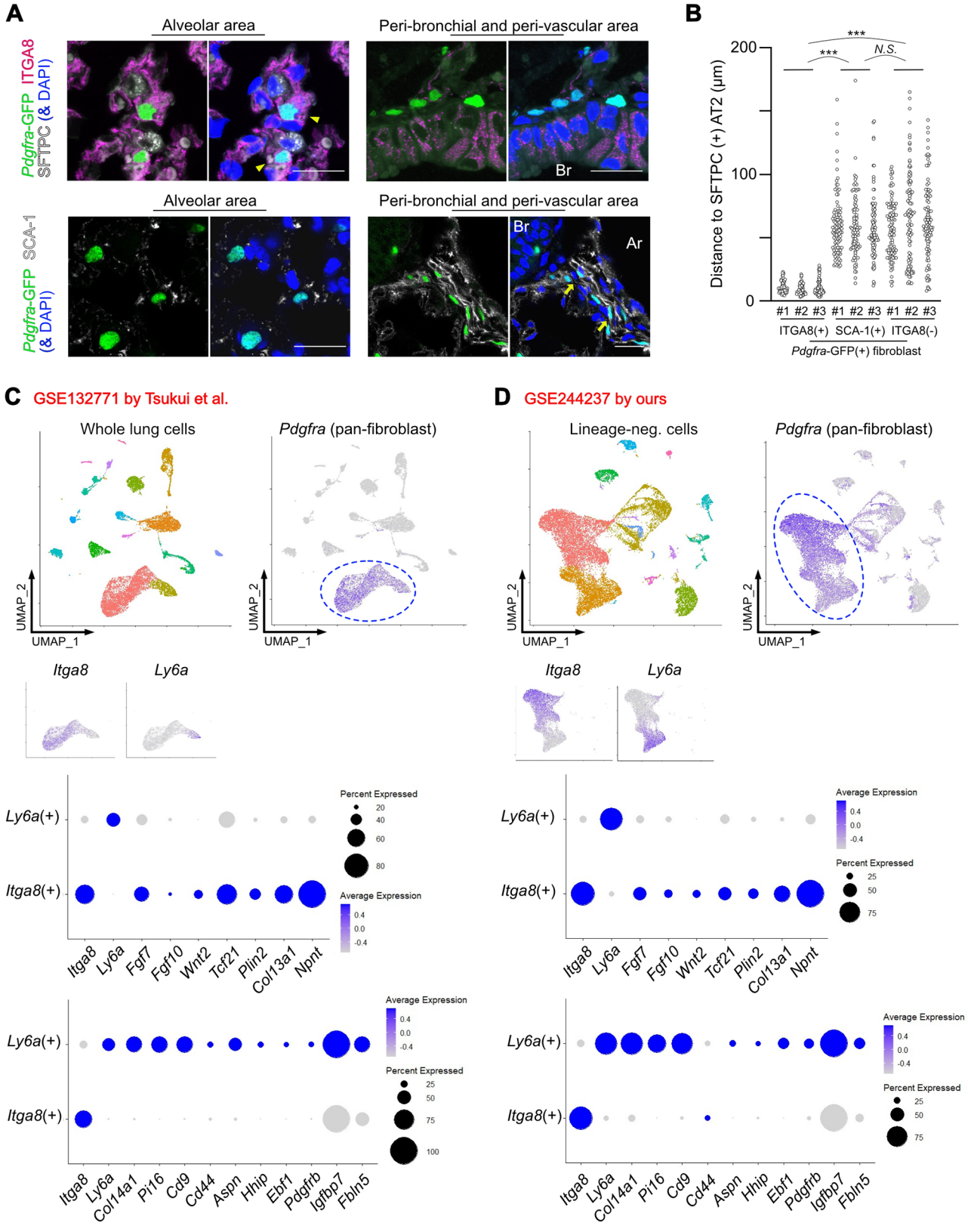

Fig. 3 (See legend on next page.)

(See figure on previous page.)

Fig. 3 Localization and transcriptome profiles of ITGA8$^+$or SCA-1$^+$lung fibroblasts. (**A**) Representative images of a *Pdgfra-GFP* mouse lung stained with anti-ITGA8 antibody (*upper*)/anti-SCA-1 antibody (*lower*), anti-SFTPC antibody (*upper*), and DAPI (*scale bars: 20 μm*). Triangles show ITGA8$^+$GFP$^+$ fibroblasts. Arrows show SCA-1$^+$GFP$^+$ fibroblasts. Br = bronchus; Ar = artery. The results are obtained from three independent adult male mice. (**B**) Quantifications of the distances from the nearest SFTPC-positive alveolar epithelial cell type 2 (AT2) in ITGA8-positive, SCA-1-positive, or ITGA8-negative fibroblasts. One hundred fibroblasts in each fibroblast subpopulation of the mouse lung are counted and the data are obtained from three independent *Pdgfra-GFP* mice (#1, #2, and #3). ***$P < 0.001$ (one-way analysis of variance with Bonferroni correction). (**C**) Reanalysis of single cell RNA-seq data of mouse lung cells isolated from *Col1a1-GFP* mice (GSE132771). Clustering of subpopulations (*left upper*) and visualization of mRNA expressions of *Pdgfra*, *Itga8*, and *Ly6a*. The lower panels show the dot plot analysis for selected genes between *Ly6a*$^+$ and *Itga8*$^+$ fibroblasts. (**D**) Analysis of our original single cell RNA-seq data of mouse lung mesenchymal cells isolated from wild-type mice (GSE244237). Clustering of subpopulations (*left upper*) and visualization of mRNA expressions of *Pdgfra*, *Itga8*, and *Ly6a*. The lower panels show the dot plot analysis for selected genes between *Ly6a*$^+$ and *Itga8*$^+$ fibroblasts

while ITGA8-single-positive fibroblasts did support alveolar organoid formation, unexpectedly, the number and size of organoids were lower than those made by SCA-1-single-positive and double-positive fibroblasts (Fig. 4B and C). These observations were almost reproduced even using wild-type lung fibroblasts (Supplementary Fig. 7A). In contrast, cultured AT2-derived cells, re-sorted by FACS using the positivity of Tomato fluorescence, exhibited no apparent differences in the expression of proliferating marker *Mki67* or major epithelial markers including *Epcam* (a pan-epithelial marker), *Sftpc* (a canonical AT2 marker), *Pdpn* (a canonical AT1 marker), and *Krt8* (an AT2-to-AT1 intermediate marker) (Fig. 4D).

Relevance with human lung resident fibroblasts

In human lungs, we have previously reported that ITGA8 is broadly expressed in lung fibroblasts at not only alveolar region but also peri-bronchiolar region [18]. It is unclear whether these human ITGA8$^+$ lung fibroblasts actually have lipid in their cytoplasm. Using frozen lung sections from six human adult subjects, we evaluated the presence of intra-cellular lipid using LipidTOX. However, there was no evidence of lipid droplets in the lung cells including fibroblasts (*data not shown*).

Using a published dataset of scRNA-seq of human lung cells [12], we evaluated the transcriptional profile of ITGA8$^+$ human lung fibroblasts. Lung resident fibroblasts with high expression of *PDGFRA* were divided into two major subpopulations: *ITGA8*-high and *ITGA8*-low fibroblasts (Fig. 5A). Interestingly, although not so apparent, *ITGA8*-high fibroblasts showed relatively higher expression of lipofibroblast markers, *LPL* and *TCF21*, than *ITGA8*-low fibroblasts. This means that *ITGA8* can be a marker of lipofibroblast-like cells even in human lungs.

Discussion

In this study, it was demonstrated that ITGA8 serves as a novel and valuable cell surface marker for alveolar lipofibroblasts within PDGFRα$^+$ total lung resident fibroblasts. By leveraging two scRNA-seq datasets, the relationship between *Itga8*$^+$ and *Ly6a*$^+$ fibroblasts and several subpopulations previously proposed in other studies was estimated. While the transcriptome profile of ITGA8 (*Itga8*)$^+$ fibroblasts, along with their close proximity to AT2 in vivo, suggests a potential role as an alveolar stem cell niche, their supporting capacity for AT2 evaluated by an alveolar organoid assay revealed an inferiority to SCA-1 (*Ly6a*)$^+$ fibroblasts. These findings contribute to advancing our understanding of lung fibroblast heterogeneity and functional distinctions.

Alveolar lipofibroblasts have a potential to transfer lipids to AT2 cells, aiding in surfactant synthesis, and are known to be part of the *Tcf21* lineage in mouse development [13, 15]. Recent scRNA-seq analyses have suggested the presence of lipofibroblast-like cells even in humans [11, 16], although we could not find the actual lipid droplets in human lungs. In vitro assessment of target cell nature, often requiring live cell isolation methods like FACS, has been hindered by the lack of suitable cell surface markers for this population. In this study, we have identified ITGA8 as the most reliable cell surface marker for alveolar lipofibroblasts, a finding validated through scRNA-seq analysis, flowcytometry, and the direct visualization of intracellular lipid content. Moreover, we showed that this method is applicable to wild-type mice of all ages, adding to its practicality.

Recent research by several investigators has highlighted the heterogeneity of lung resident fibroblasts or mesenchymal cells, and they have defined subpopulations based on their transcriptome datasets [7–12]. However, it remains unclear how these studies overlap or differ. In our present study, we aimed to comprehend the heterogeneity of lung fibroblasts using just two markers, ITGA8 and SCA-1. We also sought to establish connections with previously-reported fibroblast subpopulations (Fig. 3 and Supplementary Figs. 3 and 5), although not all subpopulations could be incorporated. We propose that PDGFRα$^+$ total lung resident fibroblasts can be categorized into at least two major subpopulations: ITGA8$^+$ alveolar lipofibroblasts and SCA-1$^+$ peri-bronchial/perivascular fibroblasts with limited lipid content (Fig. 5B).

Compared to SCA-1$^+$ fibroblasts, ITGA8$^+$ fibroblasts showed higher mRNA expressions of AT2-supportive factors: *Fgf10*, *Fgf7*, and *Wnt2* [9, 25–27]. These features, in conjunction with the localization data, evoke a similarity of ITGA8$^+$ fibroblasts with the MANC population reported by Zepp et al. [8]. However, surprisingly, the

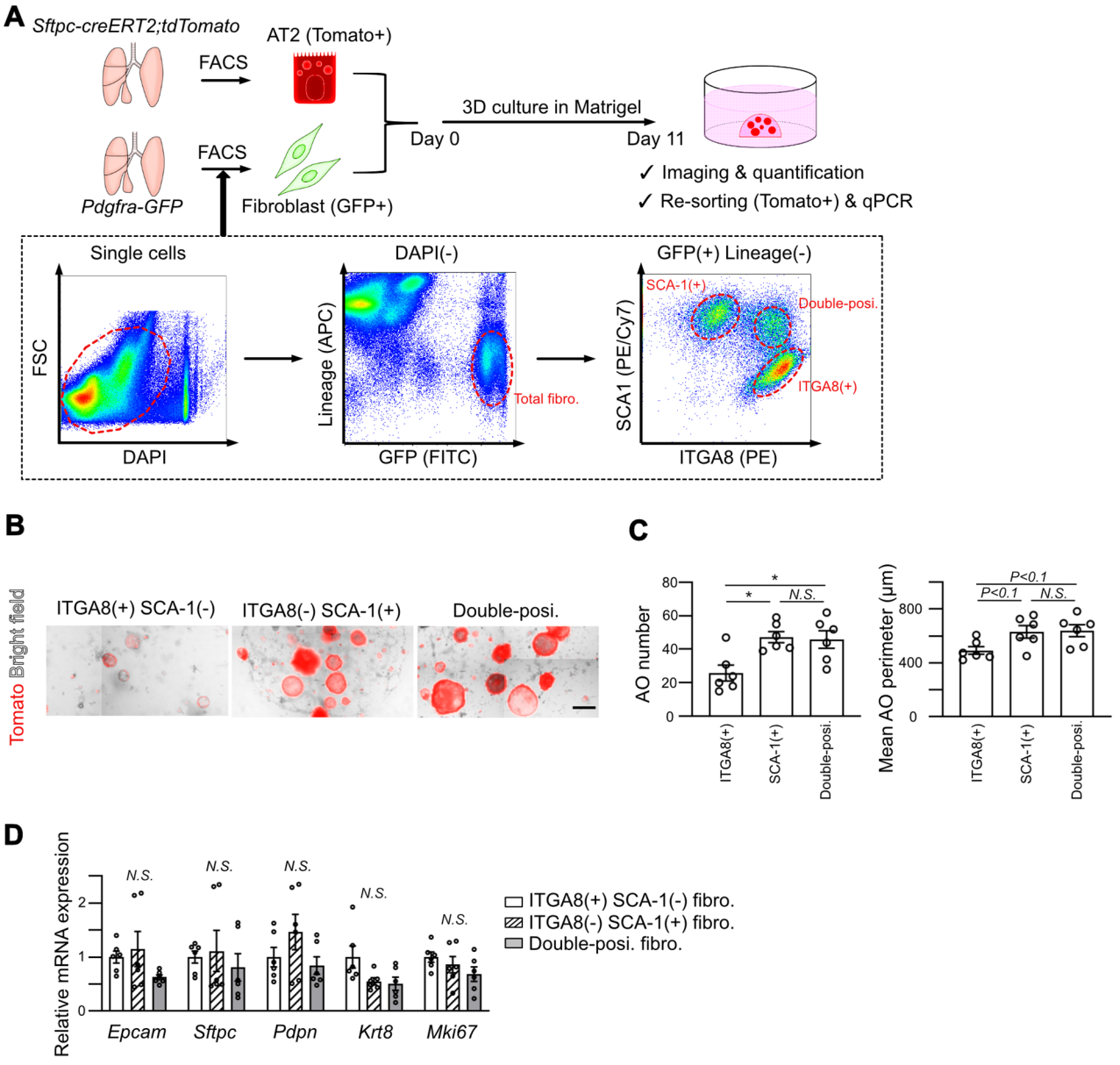

Fig. 4 Comparison of AT2-supportive capacity between subpopulations of lung fibroblasts in vitro (using *Pdgfra-GFP*mice). (**A**) Diagram of the experiments and the representative FACS panels for dividing fibroblasts into three subpopulations. (**B**) Representative images of alveolar organoids (culture day 11) made from 800 AT2 cells and 4000 lung fibroblasts (*scale bar: 500 μm*). The results are obtained from six independent adult male tamoxifen-treated *Sftpc-creERT2; tdTomato* mice (for AT2 cells) and six independent adult male *Pdgfra-GFP* mice (for fibroblasts). (**C**) Quantifications of the number (*left*) and perimeter (*right*) of alveolar organoids (AOs). Data represent the mean ± SEM of results obtained from six independent adult male mouse pairs as above. **P* < 0.05 (one-way analysis of variance with Bonferroni correction). (**D**) Comparison of mRNA expression levels by qRT-PCR for AT2-derived Tomato$^+$ cells co-cultured with lung fibroblasts in each subpopulation. Data represent the mean ± SEM of results obtained from six independent mouse pairs as above. Statistical analyses were performed using one-way analysis of variance with Bonferroni correction

supporting capacity of ITGA8$^+$ fibroblasts was inferior to SCA-1-positive fibroblasts in vitro, which is inconsistent with the data of MANC. In contrast, our observation is partly consistent with the data of SCA-1$^+$*Fgf10*$^+$ mesenchymal cell population reported by Taghizadeh et al., [9] although it seems to be further modified when considering the positive selection using PDGFRα and dead cell exclusion (Supplementary Fig. 7C, D, and E). Supporting AT2 is highly important to maintain alveolus and the functional redundancy of fibroblast subpopulation may be advantageous for the organisms. If the intracellular lipid droplets can be acquired via a differentiation process of fibroblasts, the SCA-1$^+$ peri-bronchial/perivascular fibroblasts may have a more progenitor status

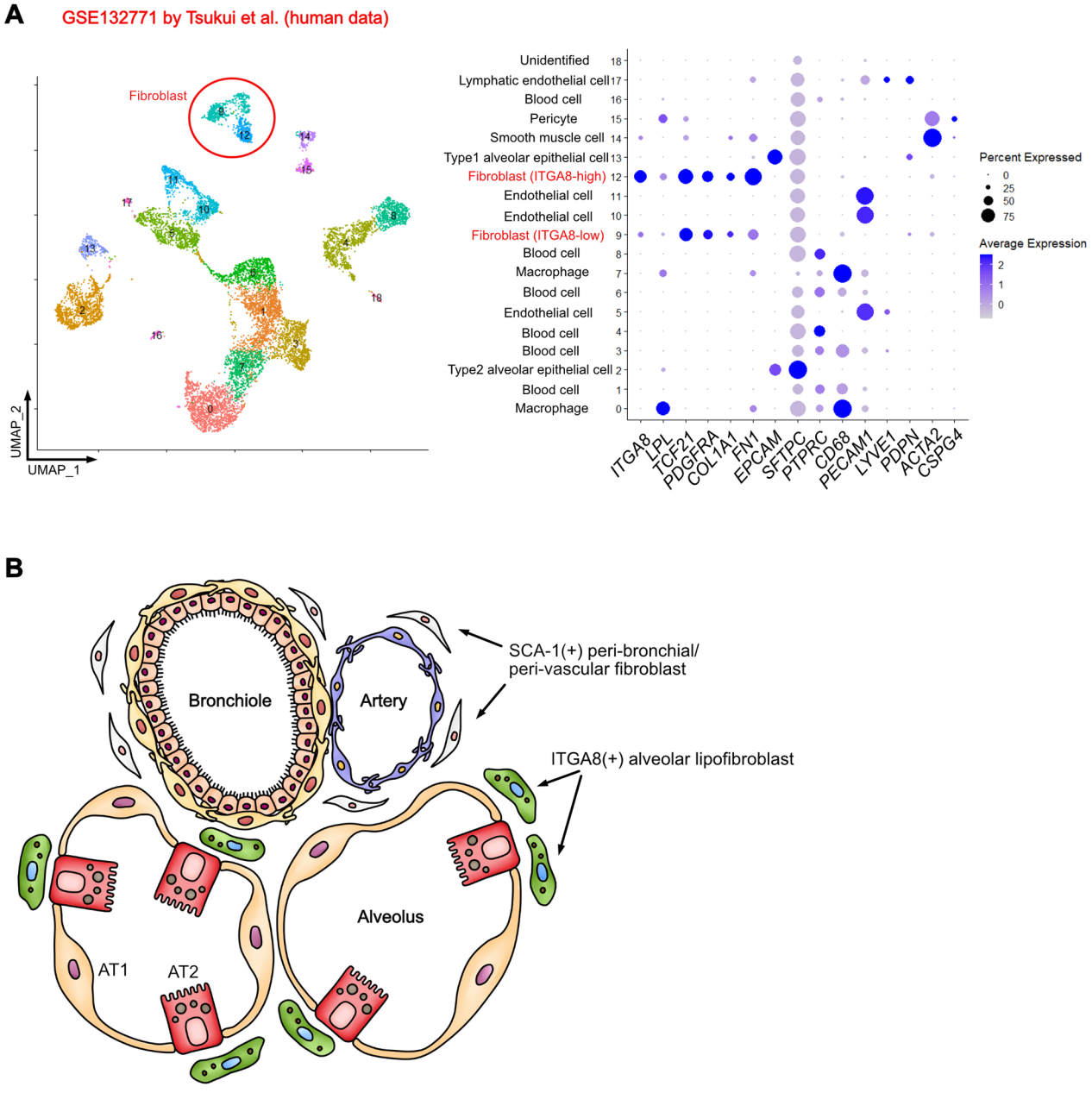

Fig. 5 Transcriptome profiles of human healthy lung cells and schema of the localization of mouse lung fibroblast subpopulations. (**A**) Reanalysis of single cell RNA-seq data of human healthy lung cells (GSE132771). Clustering of subpopulations (*left*) and the dot plot analysis for selected genes (*right*) are shown. (**B**) Schematic depiction showing the localization of mouse lung fibroblast subpopulations: ITGA8-positive and SCA-1-positive fibroblasts

than the ITGA8$^+$ alveolar fibroblasts, which was also supported by the result of our RNA velocity analysis (Supplementary Fig. 6). This hypothesis may explain the broad niche capacity of SCA-1$^+$ peri-bronchial/peri-vascular fibroblasts even for "alveolar" epithelium, although it might be just due to the in vitro higher proliferating capacity of SCA-1$^+$ fibroblasts [18], which could compensate for the capacity gap at the single cell level. Anyway, our data can be an alert to the scientific field: while single cell transcriptomics can predict cellular heterogeneity, independent validation such as by using organoid assays is equally important to determine whether genetic heterogeneity also translates into functional heterogeneity.

In summary, we identified that ITGA8$^+$ lung fibroblasts correspond to alveolar lipofibroblasts. Their biological significance and functional distinction from other fibroblast subpopulations should be further examined in the future.

Supplementary Information

The online version contains supplementary material available at https://doi.org/10.1186/s12931-025-03103-1.

Supplementary Material 1

Acknowledgements
We thank our lab members (Mr. Kurita, Mr. Endo, Ms. Kawashima, Ms. Muranaka, Ms. Honma, and Ms. Nishizawa) for their technical support.

Author contributions
A.F., Y.E., and T.I. conceived the project. A.F. and Y.E. conducted experiments and processed data. A.F., Y.E., R.H., Y.A., S.M., H.K., I.K., T.F., N.E., N.I., T.S., and T.I. interpreted results. Y.E. wrote the original manuscript. All authors reviewed the manuscript and approved the submission.

Funding
This work was supported by Grants-in-Aid for Scientific Research C (grant numbers: 21K06947 (TI); 24K11361 (YE)) from the Japan Society for the Promotion of Science. The funder provided financial support to the study, but was not involved in the design of the study, the collection, analysis, and interpretation of data, or in the writing of the manuscript.

Data availability
The authors declare that all data supporting the findings of this study are available within the article and its supplementary materials. Our original sequencing data in this study are available at NCBI GEO under the accession numbers GSE244237. Previously published sequencing data that were reanalyzed are available under the accession number GSE132771 (mouse: integrated data of GFP+ and GFP- cells; human: integrated data of "NML1_ALL", "NML2_ALL", and "NML3_ALL").

Declarations

Ethics approval and consent to participate
We handled the mice in accordance with the ethics guidelines of the institute. All the experiments in this study have been approved by Hamamatsu University School of Medicine (Approved numbers: 14–365, 22 – 021, 23–066, and 2023042).

Consent for publication
Not applicable.

Competing interests
The authors declare no competing interests.

Received: 3 September 2024 / Accepted: 6 January 2025
Published online: 13 January 2025

References

1. Plikus MV, Wang X, Sinha S, Forte E, Thompson SM, Herzog EL, et al. Fibroblasts: origins, definitions, and functions in health and disease. Cell. 2021;184(15):3852–72.
2. Zhang X, Shi X, Xie F, Liu Y, Wei X, Cai Y, et al. Dissecting pulmonary fibroblasts heterogeneity in lung development, health and diseases. Heliyon. 2023;9(9):e19428.
3. Enomoto Y, Matsushima S, Shibata K, Aoshima Y, Yagi H, Meguro S, et al. LTBP2 is secreted from lung myofibroblasts and is a potential biomarker for idiopathic pulmonary fibrosis. Clin Sci (Lond). 2018;132(14):1565–80.
4. Barkauskas CE, Cronce MJ, Rackley CR, Bowie EJ, Keene DR, Stripp BR, et al. Type 2 alveolar cells are stem cells in adult lung. J Clin Invest. 2013;123(7):3025–36.
5. Yao C, Guan X, Carraro G, Parimon T, Liu X, Huang G, et al. Senescence of alveolar type 2 cells Drives Progressive Pulmonary Fibrosis. Am J Respir Crit Care Med. 2021;203(6):707–17.
6. Enomoto Y, Katsura H, Fujimura T, Ogata A, Baba S, Yamaoka A, et al. Autocrine TGF-beta-positive feedback in profibrotic AT2-lineage cells plays a crucial role in non-inflammatory lung fibrogenesis. Nat Commun. 2023;14(1):4956.
7. Lee JH, Tammela T, Hofree M, Choi J, Marjanovic ND, Han S, et al. Anatomically and functionally distinct lung mesenchymal populations marked by Lgr5 and Lgr6. Cell. 2017;170(6):1149–e6312.
8. Zepp JA, Zacharias WJ, Frank DB, Cavanaugh CA, Zhou S, Morley MP, et al. Distinct mesenchymal lineages and niches promote epithelial Self-Renewal and Myofibrogenesis in the lung. Cell. 2017;170(6):1134–e4810.
9. Taghizadeh S, Heiner M, Vazquez-Armendariz AI, Wilhelm J, Herold S, Chen C, et al. Characterization in mice of the resident mesenchymal niche maintaining AT2 stem cell proliferation in homeostasis and disease. Stem Cells. 2021;39(10):1382–94.
10. Xie T, Wang Y, Deng N, Huang G, Taghavifar F, Geng Y, et al. Single-cell deconvolution of Fibroblast Heterogeneity in Mouse Pulmonary Fibrosis. Cell Rep. 2018;22(13):3625–40.
11. Liu X, Rowan SC, Liang J, Yao C, Huang G, Deng N, et al. Categorization of lung mesenchymal cells in development and fibrosis. iScience. 2021;24(6):102551.
12. Tsukui T, Sun KH, Wetter JB, Wilson-Kanamori JR, Hazelwood LA, Henderson NC, et al. Collagen-producing lung cell atlas identifies multiple subsets with distinct localization and relevance to fibrosis. Nat Commun. 2020;11(1):1920.
13. McGowan SE, Torday JS. The pulmonary lipofibroblast (lipid interstitial cell) and its contributions to alveolar development. Annu Rev Physiol. 1997;59:43–62.
14. Tahedl D, Wirkes A, Tschanz SA, Ochs M, Muhlfeld C. How common is the lipid body-containing interstitial cell in the mammalian lung? Am J Physiol Lung Cell Mol Physiol. 2014;307(5):L386–94.
15. Park J, Ivey MJ, Deana Y, Riggsbee KL, Sorensen E, Schwabl V, et al. The Tcf21 lineage constitutes the lung lipofibroblast population. Am J Physiol Lung Cell Mol Physiol. 2019;316(5):L872–85.
16. Travaglini KJ, Nabhan AN, Penland L, Sinha R, Gillich A, Sit RV, et al. A molecular cell atlas of the human lung from single-cell RNA sequencing. Nature. 2020;587(7835):619–25.
17. Varisco BM, Ambalavanan N, Whitsett JA, Hagood JS. Thy-1 signals through PPARgamma to promote lipofibroblast differentiation in the developing lung. Am J Respir Cell Mol Biol. 2012;46(6):765–72.
18. Matsushima S, Aoshima Y, Akamatsu T, Enomoto Y, Meguro S, Kosugi I, et al. CD248 and integrin alpha-8 are candidate markers for differentiating lung fibroblast subtypes. BMC Pulm Med. 2020;20(1):21.
19. Hamilton TG, Klinghoffer RA, Corrin PD, Soriano P. Evolutionary divergence of platelet-derived growth factor alpha receptor signaling mechanisms. Mol Cell Biol. 2003;23(11):4013–25.
20. Rock JR, Barkauskas CE, Cronce MJ, Xue Y, Harris JR, Liang J, et al. Multiple stromal populations contribute to pulmonary fibrosis without evidence for epithelial to mesenchymal transition. Proc Natl Acad Sci U S A. 2011;108(52):E1475–83.
21. Madisen L, Zwingman TA, Sunkin SM, Oh SW, Zariwala HA, Gu H, et al. A robust and high-throughput cre reporting and characterization system for the whole mouse brain. Nat Neurosci. 2010;13(1):133–40.
22. Fujimura T, Enomoto Y, Katsura H, Ogawa T, Baba S, Ogata A, et al. Identifying a lung stem cell subpopulation by combining single-cell morphometrics, Organoid Culture, and Transcriptomics. Stem Cells. 2023;41(8):809–20.
23. La Manno G, Soldatov R, Zeisel A, Braun E, Hochgerner H, Petukhov V, et al. RNA velocity of single cells. Nature. 2018;560(7719):494–8.
24. Bergen V, Lange M, Peidli S, Wolf FA, Theis FJ. Generalizing RNA velocity to transient cell states through dynamical modeling. Nat Biotechnol. 2020;38(12):1408–14.
25. Katsura H, Sontake V, Tata A, Kobayashi Y, Edwards CE, Heaton BE, et al. Human lung stem cell-based alveolospheres provide insights into SARS-CoV-2-Mediated Interferon responses and pneumocyte dysfunction. Cell Stem Cell. 2020;27(6):890–904. e8.
26. Nabhan AN, Brownfield DG, Harbury PB, Krasnow MA, Desai TJ. Single-cell wnt signaling niches maintain stemness of alveolar type 2 cells. Science. 2018;359(6380):1118–23.

27. Yuan T, Volckaert T, Chanda D, Thannickal VJ, De Langhe SP. Fgf10 Signaling in Lung Development, Homeostasis, Disease, and Repair after Injury. Front Genet. 2018;9:418.

Publisher's note